Available online at www.sciencedirect.com
ScienceDirect
Journal of Magnetic Resonance 188 (2007) 267–274
JMR Journal of Magnetic Resonance
www.elsevier.com/locate/jmr

Efficient cross polarization with simultaneous adiabatic frequency sweep on the source and target channels

Weng Kung Peng *, Kazuyuki Takeda

Division of Advanced Electronics and Optical Science, Graduate School of Engineering Science, Osaka University, Toyonaka, Osaka 560-8531, Japan

Received 13 April 2007; revised 21 June 2007
Available online 3 August 2007

Abstract

In this work, we propose a new and efficient heteronuclear cross polarization scheme, in which adiabatic frequency sweeps from far off-resonance toward on-resonance are applied simultaneously on both the source and target spins. This technique, which we call as Simultaneous ADIabatic Spin-locking Cross Polarization (SADIS CP), is capable of efficiently locking both the source and target spins with moderate power even in the presence of large spectral distribution and fast relaxation. It is shown that by keeping the time-dependent Hartmann–Hahn mismatch minimal throughout the mixing period, polarization transfer can be accelerated. Experiments are demonstrated in a powder sample of L-alanine.

Keywords: Cross polarization; Simultaneous adiabatic frequency sweep; Spin–lattice relaxation time in the rotating frame; Time-dependent Hartmann–Hahn mismatch

1. Introduction

Cross polarization (CP) [1,2] is routinely used in solid-state nuclear magnetic resonance spectroscopy to enhance the sensitivity of nuclear spins (S spins) with relatively low gyromagnetic ratio, by transferring the larger polarization of nuclear spins (I spins) such as ^{1}H.

The original CP technique [2] employs a $\frac{\pi}{2}$ pulse at I followed by simultaneous irradiations at I and S so that the Hartmann–Hahn condition is satisfied. Since 1990s, a lot of modifications to the pulse sequence have been proposed to improve the efficiency of polarization transfer. For example, under high-speed MAS [3–7], the Hartmann–Hahn matching profile splits into sidebands. As a result, efficiency of the polarization transfer becomes sensitive to the mismatch of the rf amplitudes. In order to make transfer robust against the mismatch, a number of techniques [8–15] have been proposed which employ modulation of rf amplitude or frequency during the contact time. They include Amplitude-Modulated Cross Polarization (AMCP) [8], Adiabatic Passage through the Hartmann–Hahn condition (APHH) [9–11], Amplitude-Modulated Adiabatic Passage Cross Polarization (AMAP-CP) [12], Ramped-Amplitude Cross Polarization (RAMP-CP) [13], Hartmann–Hahn matching via adiabatic frequency sweep [14], sinusoidally frequency-modulated cross polarization [15], and so forth. Since the magnitude of the effective field in the rotating frame changes in time, the Hartmann–Hahn condition can be made to be fulfilled on the way during the contact time.

Another viewpoint for improving the CP performance has recently been put forth, in which the efficiency of spin-locking is enhanced while the favorable properties of the modulation schemes are still retained. In the proposed technique, referred to as Nuclear Integrated Cross Polarization (NICP) [16], the initial $\frac{\pi}{2}$ pulse on the I spin is removed, and the frequency of the I channel is adiabatically swept from far-off resonance toward on-resonance. The far-off to on-resonance frequency sweep serves the following two purposes: (i) even in the presence of considerable spectral distribution due to chemical shift or dipolar line broadening, the I spin packets follow, i.e., locked along

* Corresponding author. Fax: +81 668506321.
E-mail address: peng@qc.ee.es.osaka-u.ac.jp (W.K. Peng).

1090-7807/$ - see front matter © 2007 Elsevier Inc. All rights reserved.
doi:10.1016/j.jmr.2007.06.015

the effective field, which is initially pointing in the z direction and gradually tilted toward the xy plane. Since it is the locked components of the I spin packets that participate in polarization transfer, this approach leads to increase in the enhancement factor when available/tolerable rf power is not large enough to flip the entire spin packets with the $\frac{\pi}{2}$ pulse in the previous CP techniques. (ii) The magnitude of the effective field takes the maximum value at the beginning of the sweep and decreases gradually. Thus, transfer is expected to be insensitive to rf-mismatch.

In order to further increase the attainable magnetization, we present in this work an improved scheme for NICP, in which adiabatic frequency sweeps from far-off resonance toward on-resonance are applied simultaneously on both the source and target spins. This technique, which we call as Simultaneous ADIabatic Spin-locking Cross Polarization (SADIS CP), has the following advantages: (i) simultaneous sweep reduces the amount of Hartmann–Hahn offset throughout the whole sequence as compared to that in NICP, therefore allowing faster polarization transfer. (ii) Offset irradiation leads to higher effective field. The higher effective field, in general, results in a longer spin–lattice relaxation time in the rotating frame. The property that the effective field is initially the largest is particularly attractive, because both the I and S magnetization can be well kept during the sequence. Offset assisted power reduction is also attractive for application to power lossy biological samples [17]. (iii) The favorable properties of NICP mentioned above are retained in this new approach. We present here, the principle behind SADIS CP and demonstrate its performance in ^{1}H–^{13}C double resonance experiments using a powder sample of L-alanine. As shown later, the above merits are more than enough to compensate the cost of the decreased I–S dipolar interaction with offset irradiation.

2. Principle

Let us consider an isolated heteronuclear spin pair $I = \frac{1}{2}$ and $S = \frac{1}{2}$ and suppose that simultaneous linear frequency sweeps are applied at both the I and S spins under rf irradiations with intensities ω_{1I} and ω_{1S}, respectively. For simplicity, homonuclear dipolar interactions among the abundant protons are neglected. We write the rotating-frame Hamiltonian as

$$H = -(\Delta\Omega_I(t) + \Omega_I)I_z - \omega_{1I}I_x - (\Delta\Omega_S(t) + \Omega_S)S_z - \omega_{1S}S_x + D(t)I_zS_z. \quad (1)$$

Here, Ω_I and Ω_S are the isotropic chemical shifts for I and S. $D(t)$ is the magnitude of the dipolar interaction between them, which is modulated by MAS and is given by

$$D(t) = d_{IS}[G_1\cos(w_r t) + G_2\cos(2w_r t)] \quad (2)$$

where w_r is the spinning frequency and G_k $(k = 1, 2)$ depends on the orientation of the internuclear vector in a reference frame fixed to the rotor. d_{IS} is the dipolar coupling constant. In the pulse sequence of SADIS CP as depicted in Fig. 1(c), the frequency-offset terms $\Delta\Omega_I$ and $\Delta\Omega_S$ change in time according to

$$\Delta\Omega_\epsilon(t) = -\Delta\omega_\epsilon\left(1 - \frac{t}{T}\right), \quad (3)$$

where $\epsilon = I$ or S, T is the period of frequency sweep, and $\Delta\omega_\epsilon$ is the frequency sweep width. Note that the special case of SADIS CP in which $\Delta\omega_S = 0$ (no frequency sweep on the S channel) corresponds to the NICP sequence described in Fig. 1(b).

We assume that the rate of frequency sweep is slow enough for both I and S and consider the doubly tilted rotating frame in which the effective fields for both spins point in the z axis. When the adiabatic conditions are met, transformation from the rotating frame into the doubly tilted rotating frame does not have significant effects on the density matrix, whereas the Hamiltonian H^{TR} in this new frame is given by

$$H^{TR} = H_Z + H_D, \quad (4)$$

where

$$H_Z = \omega_{eI}(t)I_z + \omega_{eS}(t)S_z \quad (5)$$

$$H_D = D(t)[I_z\cos(\alpha_I(t)) + I_x\sin(\alpha_I(t))][S_z\cos(\alpha_S(t)) + S_x\sin(\alpha_S(t))], \quad (6)$$

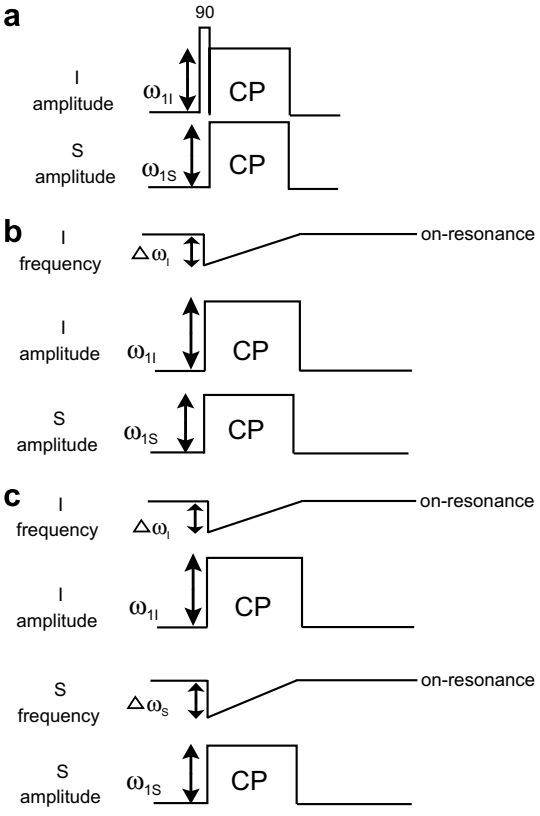

Fig. 1. Pulse sequences for (a) the conventional CP, (b) NICP, and (c) SADIS CP.

with

$$\omega_{e\epsilon}^2(t) = \omega_{1\epsilon}^2 + (\Delta\Omega_\epsilon(t) + \Omega_\epsilon)^2, \tag{7}$$

and

$$\alpha_\epsilon(t) = \tan^{-1}\frac{\omega_{1\epsilon}(t)}{\Delta\Omega_\epsilon(t) + \Omega_\epsilon}. \tag{8}$$

The evolution of the system is governed by the propagator $U(t)$ given by

$$U(t) = T\exp\left[\int_0^t \mathrm{d}t' H^{\mathrm{TR}}\right] = U_0(t)U_1(t), \tag{9}$$

where

$$U_0(t) = T\exp\left[\int_0^t \mathrm{d}t' H_Z\right], \tag{10}$$

$$U_1(t) = T\exp\left[\int_0^t \mathrm{d}t' \widetilde{H}_D\right], \tag{11}$$

with

$$\begin{aligned}\widetilde{H}_D &= U_0^{-1}(t)H_D U_0(t) \qquad (12)\\ &= D(t)[S_z\cos(\alpha_S(t)) + (S_x\cos(\omega_{eS}t)\\ &\quad - S_y\sin(\omega_{eS}t))\sin(\alpha_S(t))][I_z\cos(\alpha_I(t))\\ &\quad + (I_x\cos(w_{eI}t) - I_y\sin(w_{eI}t))\sin(\alpha_I(t))]. \qquad (13)\end{aligned}$$

When the time-dependent Hartmann–Hahn condition

$$\Delta_{\mathrm{HH}}(t) \equiv \omega_{eI}(t) - \omega_{eS}(t) - nw_r = 0, (n = -2, -1, 1, 2) \tag{14}$$

is satisfied, interference between the spatial and spin parts in $\widetilde{H}_D$ leads to the non-vanishing average Hamiltonian

$$\overline{\widetilde{H}}_D = \frac{1}{8}d_{IS}G_n\sin\alpha_I(t)\sin\alpha_S(t)(I_+S_- + I_-S_+). \tag{15}$$

In order to discuss the exchange of the spin states between I and S, we focus on the zero-quantum (ZQ) subspace spanned by states $|+-\rangle$ and $|-+\rangle$, in which the secular Hamiltonian H^{ZQ} is represented by

$$H^{\mathrm{ZQ}} = 2\Delta_{\mathrm{HH}}(t)I_z^{\mathrm{ZQ}} + \frac{1}{4}D_{\mathrm{eff}}(t)I_x^{\mathrm{ZQ}}, \tag{16}$$

where $D_{\mathrm{eff}}(t)$, which we call the effective dipolar frequency, is given by

$$D_{\mathrm{eff}}(t) = d_{IS}G_n\sin\alpha_I(t)\sin\alpha_S(t), \tag{17}$$

and I_z^{ZQ} and I_x^{ZQ} are the ZQ fictitious spin $-\frac{1}{2}$ operators given by

$$I_z^{\mathrm{ZQ}} = \frac{1}{2}[|+-\rangle\langle+-| - |-+\rangle\langle-+|], \tag{18}$$

$$I_x^{\mathrm{ZQ}} = \frac{1}{2}[|+-\rangle\langle-+| + |-+\rangle\langle+-|]. \tag{19}$$

We assume that initially the state $|+-\rangle$ is idempotently populated, so that the ZQ density matrix $\rho^{\mathrm{ZQ}}(t=0)$ is

$$\rho^{\mathrm{ZQ}}(t=0) = \begin{pmatrix}1 & 0\\ 0 & 0\end{pmatrix} = \frac{1}{2}\mathbf{1} + I_Z^{\mathrm{ZQ}}. \tag{20}$$

When the I and S spins have exchanged their spin states, the density matrix would be

$$\rho^{\mathrm{ZQ}}(t=ct) = \begin{pmatrix}0 & 0\\ 0 & 1\end{pmatrix} = \frac{1}{2}\mathbf{1} - I_Z^{\mathrm{ZQ}}. \tag{21}$$

Hence, the transverse magnetization $\langle S_x\rangle$ of the S spin is correlated with $\langle I_Z^{\mathrm{ZQ}}\rangle$ through

$$\begin{aligned}\langle S_x\rangle(t) &= \frac{1}{2} - \langle I_Z^{\mathrm{ZQ}}\rangle \qquad (22)\\ &= \frac{1}{2} - \mathrm{Tr}[I_Z^{\mathrm{ZQ}}\rho^{\mathrm{ZQ}}(t)]. \qquad (23)\end{aligned}$$

Since the problem has now been reduced to the two-level system, geometric state representation is possible, i.e., a general state ρ^{ZQ} in the ZQ-subspace is given by employing a vector $\mathbf{M}$ as

$$\rho^{\mathrm{ZQ}}(t) = M_x(t)I_x^{\mathrm{ZQ}} + M_y(t)I_y^{\mathrm{ZQ}} + M_z(t)I_z^{\mathrm{ZQ}}, \tag{24}$$

and the dynamics of $\mathbf{M}$ is governed by the Bloch equation [18]

$$\frac{\mathrm{d}}{\mathrm{d}t}\mathbf{M} = \mathbf{M}\times\omega_{\mathrm{eff}}^{\mathrm{ZQ}}, \tag{25}$$

where $\omega_{\mathrm{eff}}^{\mathrm{ZQ}}$ is the vector of effective field in the ZQ-subspace which is represented by

$$\omega_{\mathrm{eff}}^{\mathrm{ZQ}} = \begin{pmatrix}(\omega_{\mathrm{eff}}^{\mathrm{ZQ}})_x\\ (\omega_{\mathrm{eff}}^{\mathrm{ZQ}})_y\\ (\omega_{\mathrm{eff}}^{\mathrm{ZQ}})_z\end{pmatrix} = \begin{pmatrix}\frac{1}{4}D_{\mathrm{eff}}(t)\\ 0\\ 2\Delta_{\mathrm{HH}}(t)\end{pmatrix}. \tag{26}$$

Substituting Eq. (26) into Eq. (25), we arrive at

$$\frac{\mathrm{d}}{\mathrm{d}t}\begin{pmatrix}M_x\\ M_y\\ M_z\end{pmatrix} = \begin{pmatrix}2\Delta_{\mathrm{HH}}(t)M_y\\ \frac{1}{4}D_{\mathrm{eff}}(t)M_z - 2\Delta_{\mathrm{HH}}(t)M_x\\ -\frac{1}{4}D_{\mathrm{eff}}(t)M_y\end{pmatrix}\begin{pmatrix}M_x\\ M_y\\ M_z\end{pmatrix}. \tag{27}$$

In order to make a simple comparison on transfer efficiencies between SADIS CP and NICP, we consider one specific crystallite orientation in a static sample. We also neglect the effect of relaxation here, which will be discussed later. Assuming the initial magnetization $(0,0,1)$, we evaluated numerically (Fig. 2) the dynamics of the S magnetization for an arbitrarily given set of parameters $\left(\frac{\omega_{1S}}{2\pi} = 35\ \mathrm{kHz}, \frac{\omega_{1I}}{2\pi} = 40\ \mathrm{kHz}, \frac{\Delta\omega_I}{2\pi} = 80\ \mathrm{kHz}, T = 2\ \mathrm{ms}, \text{ and } \frac{d_{IS}}{2\pi} = 45\ \mathrm{kHz}\right)$. The difference between SADIS CP (blue line) and NICP (green line) is the application of the frequency sweep on the S channel, in which $\frac{\Delta\omega_S}{2\pi} = 90$ kHz for SADIS CP while $\frac{\Delta\omega_S}{2\pi} = 0$ kHz for NICP.

As shown in Fig. 2, the calculated buildup of the S magnetization is faster in SADIS CP than in NICP. Thus, the same amount of S polarization can be achieved with SADIS CP in a relatively shorter period of time as compared to NICP. This feature is particularly attractive for spins with short relaxation times, where polarization transfer should be as fast as possible before overwhelmed by the effect of relaxation. The oscillation at the I–S dipolar frequency is also visible in the build up curve. It is worth

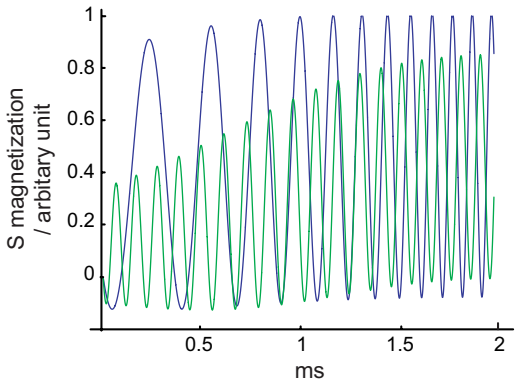

Fig. 2. Numerically calculated buildup curves for SADIS CP (blue line) and NICP (green line). $\frac{\Delta\omega_S}{2\pi} = 90$ kHz and $\frac{\Delta\omega_S}{2\pi} = 0$ were used for SADIS CP and NICP, respectively. Other parameters were $\frac{\omega_{1S}}{2\pi} = 35$ kHz, $\frac{\omega_{1I}}{2\pi} = 40$ kHz $\frac{\Delta\omega_I}{2\pi} = 80$ kHz, and $T = 2$ ms. (For interpretation of the references to color in this figure legend, the reader is referred to the web version of this paper.)

noting here that the effective dipolar frequency $D_{\text{eff}}(t)$ given in Eq. (17) is lower in SADIS CP than in NICP by the scaling factor $\sin\alpha_S(t)$. For this reason, NICP shows faster oscillation than SADIS CP, as revealed in Fig. 2. In NICP, however, the buildup of the amplitude profile of the oscillation is rather slower because of the larger Hartmann–Hahn offset. In actual situations, this oscillation is expected to be suppressed due to distribution of the I–S dipolar frequency in powder samples, and due to the effect of homonuclear dipolar interactions among the I spins.

The efficient polarization transfer in SADIS CP is ascribed to the smaller time-dependent Hartmann–Hahn offset $\Delta_{\text{HH}}(t)$ than that in NICP throughout the sequence. In the ZQ subspace, $\Delta_{\text{HH}}(t)$ appears in the I_Z^{ZQ} term which corresponds to the resonance offset in the conventional nutation. For relatively smaller $\Delta_{\text{HH}}(t)$ as in the case of SADIS CP, the ZQ effective field is tilted more toward the xy plane. Since the inversion of the magnetization requires on-resonance nutation, polarization transfer is expected to be faster in SADIS CP. Furthermore, the aforementioned attractive features of NICP can be retained when the adjustable parameters (ω_{1S}, ω_{1I}, $\Delta\omega_I$, $\Delta\omega_S$) are appropriately chosen.

The time-dependent Hartmann–Hahn offset should be kept small as long as the Hartmann–Hahn condition is satisfied for the individual target spins. Generally speaking, experiments should be arranged in such a way that the magnitude of the effective fields are initially different, and so they are the other way around at the end of the sequence. For example, for the case of simple isolated two-spin system under sample spinning,

(1) at $t = 0$

$$\omega_{eI} + w_r \leqslant \omega_{eS} \leqslant \omega_{eI} + 2w_r, \tag{28}$$

and

(2) at $t = T$

$$\omega_{eS} + w_r \leqslant \omega_{eI} \leqslant \omega_{eS} + 2w_r, \tag{29}$$

or vice versa so that the crossing will be limited to $|n| = 1$ matching condition, where the magnitude of the dipolar coefficient is the largest. The reversal of the magnitude relation between the effective fields guarantees that the Hartmann–Hahn condition is satisfied during the simultaneous sweep.

3. Experimental

Experiments were performed at room temperature in a magnetic field of 11.7 T using a home-built triple resonance probe equipped with a Varian 4 mm spinning module. Carrier frequencies for the ^{13}C and ^{1}H channels were 125.675 and 499.789 MHz, respectively. The ^{13}C NMR signals in a polycrystallines sample of ^{13}C-labelled L-alanine were measured at a spinning frequency of 13.5 kHz under ^{1}H TPPM decoupling [19]. Recycle delays were 60 s for ^{13}C direct observation and 2 s for all other CP experiments.

4. Results and discussion

4.1. 'Contact-time'-dependent behavior

Fig. 3 shows the signal intensities of the methyl, methine, and carboxyl ^{13}C spins for various contact times

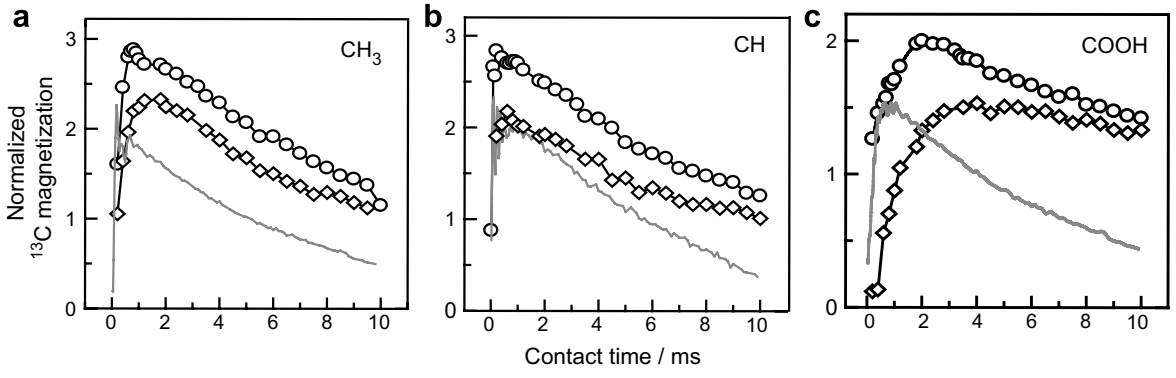

Fig. 3. ^{13}C magnetizations for (a) CH_3, (b) CH, and (c) COOH in L-alanine for various contact times measured with conventional CP (—), NICP (◇), and SADIS CP (○). The vertical axis was normalized with respect to the value obtained with direct detection. For conventional CP, $\frac{\omega_{1S}}{2\pi}$ was fixed to 45 kHz and ω_{1I} was adjusted separately so that each of the isotropic chemical shifts satisfied sideband (+1) matching condition. For SADIS CP, $\frac{\omega_{1S}}{2\pi}$ =35 kHz, $\frac{\Delta\omega_S}{2\pi}$ =110 kHz and $\frac{\omega_{1I}}{2\pi}$ =48 kHz, $\frac{\Delta\omega_I}{2\pi}$ =80 kHz. For NICP, $\frac{\Delta\omega_S}{2\pi}$ =0 kHz while the rest of the parameters are the same as SADIS CP.

in the conventional CP, NICP, and SADIS CP techniques. By 'contact time' we refer to the time interval T of the frequency-sweep for NICP and SADIS CP. The signal intensities are normalized with respect to the signal obtained in thermal equilibrium with direct excitation with sufficiently long recovery delay time of 60 s. In the conventional CP experiment, separate measurements were carried out for the individual carbon groups by setting the carrier frequency at on-resonance and adjusting the $n = +1$ Hartmann–Hahn condition, and the maximum enhancement factors recorded were 2.26, 2.32, 1.52 for the methyl, methine, and carboxyl ^{13}C spins with contact times of 0.16, 0.10, and 0.68 ms, respectively. This result indicates that it is impossible to choose a common set of optimal contact time and rf power. This problem would be more serious for samples with large chemical shift distribution or experiments under high static field where the Hartmann–Hahn matching profile is shifted according to the individual chemical shifts. The relatively smaller signal enhancement for the conventional CP is also due to less efficient spin-locking of the ^{1}H magnetization with the rf intensity of 59 kHz, which is smaller than the ^{1}H dipolar linewidth. Thus, the performance of polarization transfer in those previous CP techniques using the initial $\frac{\pi}{2}$ pulse at the I spin degrades when the available or tolerable rf power is limited. Moreover, the low rf intensity can cause fast spin–lattice relaxation in the rotating frame, as discussed below.

In NICP, it was found that comparable amount of enhancement factors (2.32, 2.27, 1.53) can be obtained in a single experiment using a common set of experimental parameters $\left(\frac{\omega_{1S}}{2\pi} = 35 \text{ kHz}, \frac{\omega_{1I}}{2\pi} = 48 \text{ kHz} \text{ and } \frac{\Delta\omega_I}{2\pi} = 80 \text{ kHz}\right)$, as demonstrated in Fig. 3. The improved performance is ascribed to the following three reasons. First, the magnitude of the initial effective field set along the z axis is much larger than the spectral distribution of the I spin. Thus, the I spin packets can be well locked along the effectively field, and therefore participate in the polarization transfer process even with moderate rf amplitudes. Second, the fact that the magnitude of the effective field changes with time permits the Hartmann–Hahn condition to be satisfied even in the presence of large spectral distribution or rf-intensity offset. Finally, the larger effective field with the off-resonance irradiation at the I channel leads to slower spin–lattice relaxation, so that larger amount of the I magnetization can be retained along the effective field before polarization transfer is completed. Since the common set of experimental parameters gave nearly the optimal enhancement factors, the sensitivity of the ^{13}C spectrum obtained with NICP (Fig. 4(b)) was considerably higher than that obtained with the conventional CP (Fig. 4(a)).

In SADIS CP, the maximum enhancement factors (2.88, 2.84, 2.00) were (24%, 25%, 31%) higher than those obtained in NICP, as demonstrated in Fig. 3. This was achieved by employing an additional frequency sweep $\left(\frac{\Delta\omega_S}{2\pi} = 110 \text{ kHz}\right)$ on the S channel while other parameters were kept the same as the optimal ones for the NICP experiment. As can also be seen in Fig. 3, the contact times that gave the maxima in SADIS CP are slightly shorter than those in NICP. This indicates that the buildup of the ^{13}C magnetizations was faster in SADIS CP, confirming the rather simplified theoretical descriptions in the previous section which neglected the homonuclear dipolar interactions among the protons. The optimized ^{13}C spectrum of SADIS CP is shown in Fig. 4(c).

For the purpose of clarifying the role of additional frequency sweep in the S channel, we have carried out related experiments, as described below.

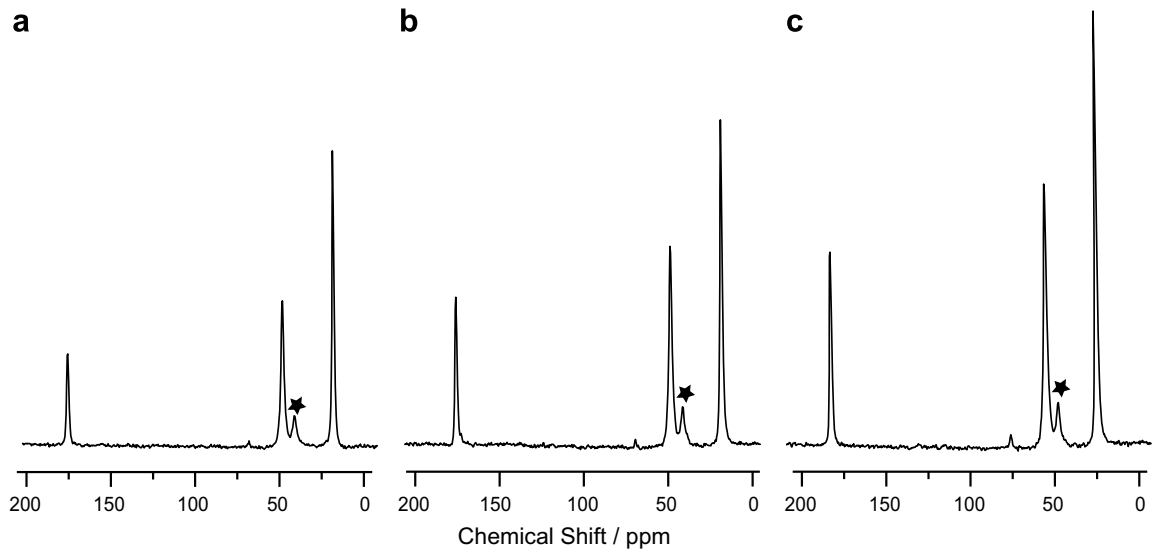

Fig. 4. ^{13}C MAS spectra of L-alanine obtained with (a) conventional CP ($\frac{\omega_{1S}}{2\pi}$ =45 kHz, $\frac{\omega_{1I}}{2\pi}$ =58.5 kHz, contact time = 0.28 ms), (b) NICP ($\frac{\omega_{1S}}{2\pi}$ =35 kHz, $\frac{\Delta\omega_S}{2\pi}$ =0 kHz, $\frac{\omega_{1I}}{2\pi}$ =48 kHz, $\frac{\Delta\omega_I}{2\pi}$ =80 kHz, and contact time = 2 ms), and (c) SADIS CP ($\frac{\omega_{1S}}{2\pi}$ =35 kHz, $\frac{\Delta\omega_S}{2\pi}$ =110 kHz, $\frac{\omega_{1I}}{2\pi}$ =48 kHz, $\frac{\Delta\omega_I}{2\pi}$ =80 kHz, and contact time = 0.8 ms), The peaks indicated by asterisks originate from impurity which was intentionally mixed for other purposes. There were no interaction between the impurity and L-alanine because it was just mechanically mixed.

4.2. ^{13}C magnetization buildup

In order to trace the buildup behavior in NICP and SADIS CP, time interruption measurements were carried out, in which frequency sweep was aborted at various moments during the contact time. Fig. 5 shows the buildup of the methine ^{13}C magnetization with $T = 1.8$ ms, $\frac{\omega_{1S}}{2\pi}$ =35 kHz, $\frac{\omega_{1I}}{2\pi}$ =52 kHz, $\frac{\Delta\omega_I}{2\pi}$ =100 kHz, and with $\frac{\Delta\omega_S}{2\pi}$ =0 and 120 kHz for NICP and SADIS CP, respectively. Unlike the simplified calculation in Fig. 2, the oscillations were suppressed due to distribution of the *IS* dipolar frequency in the powder sample used in our study, and due to the dipolar interactions among the ^{1}H spins which were neglected in the theoretical part. For NICP, the Hartmann–Hahn crossing occurred at $t \sim 1.2$ ms while for SADIS CP, the *S* magnetization surged up as the Hartmann–Hahn crossings occured at $T = 0.5$ and 1.3 ms, as demonstrated in Fig. 5. In SADIS CP, the overall attained ^{13}C magnetization was much larger than that in NICP. One reason for this result is that $\Delta_{HH}(t)$ is smaller throughout the sequence in SADIS CP, which leads to the following two consequences. First, the chance of Hartmann–Hahn crossing increase when $\Delta_{HH}(t)$ is small; in this example the crossing occured twice in SADIS CP while it only occured once in NICP. Second, the smaller $\Delta_{HH}(t)$, the higher the rate of polarization transfer in each crossing. In other words, NICP requires a longer contact time to attain the same amount of polarization in SADIS CP.

In reality, however, the available time interval is limited by the effect of relaxation, which restores the spin system toward thermal equilibrium. Since the final ^{13}C magnetization is determined by the balance between the buildup and relaxation processes, both the transfer rate and the chance of the Hartmann–Hahn crossing are desirable to be maximized for a given relaxation rate. In both of these respects, SADIS CP is superior to NICP, despite that the *IS* dipolar interaction is weaker in SADIS CP by an additional scaling factor $\sin\alpha_S(t)$. Thus, SADIS CP opens its application to systems in which the effect of relaxation (particularly on the *S* spins) is so serious that the previously proposed CP techniques do not provide efficient polarization transfer. Such systems include, e.g., paramagnetic materials, samples with molecular motion whose time scale is comparable to the Larmor frequency, and samples in which the target rare spins, such as ^{13}C and ^{15}N, are isotopically enriched, because the presence of the additional homonuclear dipolar interactions among the *S* spins can reduce the relaxation time [20,21]. Application of SADIS CP to such materials is under progress.

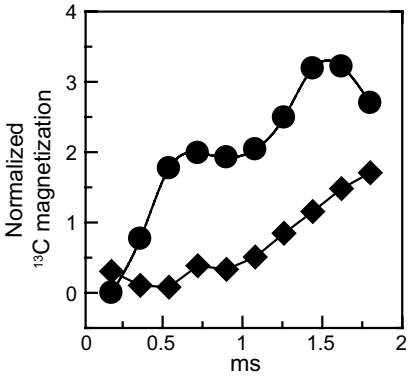

Fig. 5. Buildup behavior of the methine ^{13}C magnetization in L-alanine in SADIS CP (●) and NICP (◆) obtained with time-interruption measurements. For SADIS CP, experimental parameters were $\frac{\Delta\omega_S}{2\pi} = 120$ kHz, $\frac{\omega_{1S}}{2\pi} = 35$ kHz, $\frac{\Delta\omega_I}{2\pi} = 100$ kHz, and $\frac{\omega_{1I}}{2\pi} = 52$ kHz. For NICP, the frequency sweep for *S* channel were turned off $\left(\frac{\Delta\omega_S}{2\pi} = 0 \text{ kHz}\right)$, while the other parameters were the same as in SADIS CP. A contact time of 1.8 ms was used. A correction factor $1/\sin(\alpha_S)$ was taken into account for SADIS CP since only the projection of the magnetization onto the *xy* plane is measurable.

Moreover, SADIS CP, which make use of the offset irradiation on the *S* spins, can further suppress the effect of relaxation, because the effective field for the *S* spin is always larger throughout the sequence in SADIS CP as compared to NICP. Spin–lattice relaxation times in the rotating frame can be enhanced with offset irradiation, which suppresses the unwanted decay of the ^{13}C magnetization in the rotating frame. In particular, this is the case for the ^{13}C spins in L-alanine, as pointed by Akasaka et al. [22]. Thus, SADIS CP can spare longer 'contact' between both spins than NICP does.

4.3. Hartmann–Hahn matching profile

In order to study the efficiency of polarization transfer in terms of the Hartmann–Hahn mismatch $\Delta_{HH}(t)$ described in Eq. (14), we have examined the signal intensities of the methine ^{13}C as a function of the rf amplitude ω_{1I} for three frequency sweep widths $\frac{\Delta\omega_S}{2\pi}$ =0, 20, and 110 kHz on the *S* channel (Fig. 6(a)), which represents NICP, less optimal SADIS CP and the optimal SADIS CP, respectively. All other parameters were kept fixed. For $\frac{\Delta\omega_S}{2\pi}$ =110 kHz (black line), $\Delta_{HH}(t)$ is minimal throughout the sequence, providing the highest signal intensity and well-broadened matching profile over a wide range of rf amplitudes. For the case of $\frac{\Delta\omega_S}{2\pi}$ =20 kHz (gray line), the signal intensity dropped significantly as ω_{1I} was increased. In the case of NICP $\left(\frac{\Delta\omega_S}{2\pi} = 0 \text{ kHz}\right)$ denoted by the broken line, the signal intensity further dropped and the transfer efficiency became less robust against deviation in ω_{1I}. This is because the *I* effective field did not overlap with any of the Hartmann–Hahn matching conditions for $\frac{\omega_{1I}}{2\pi}$ beyond approximately 60 kHz (which corresponds to $\omega_{1S} + 2w_r$ condition).

Fig. 6(b) and (c) show the magnitudes of the effective fields during the SADIS CP and NICP sequences. As seen in Fig. 6(c), the Hartmann–Hahn condition is not met for the relatively stronger irradiation at the *I* spin in NICP. In SADIS CP, on the other hand, the Hartmann–Hahn crossings take place for a wide range of irradiation amplitudes at the *I* spin, as depicted in Fig. 6(b). Hence, the matching profile in SADIS CP is considerably wider than that in NICP, making the present scheme robust against

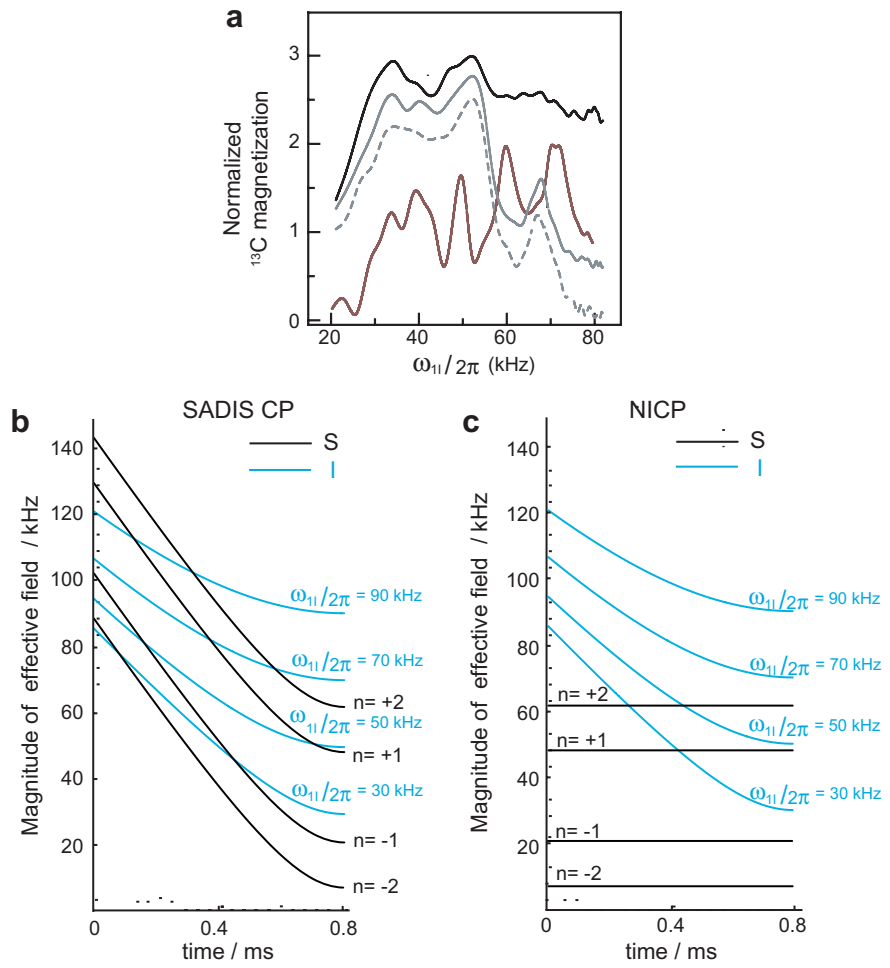

Fig. 6. (a) ω_{1I} dependence of the methine ^{13}C signal intensities in SADIS CP with (i) $\frac{\Delta\omega_S}{2\pi}$ =110 kHz (black line), (ii) $\frac{\Delta\omega_S}{2\pi}$ =20 kHz (gray line), and (iii) $\frac{\Delta\omega_S}{2\pi}$ =0 kHz (broken line). Note that (iii) corresponds to NICP, which is a special case of SADIS CP. Other parameters were fixed to $\frac{\Delta\omega_I}{2\pi} = 80$ kHz, $\frac{\omega_{1S}}{2\pi} = 35$ kHz and $T = 0.8$ ms. For comparison, the Hartmann–Hahn matching profile for the conventional CP with $\frac{\omega_{1S}}{2\pi} = 45$ kHz and $T = 0.80$ ms is also shown in brown line. (b) Time dependence of the magnitude of the effective field in SADIS CP for the S spin (black lines) and I spin (blue lines) with $T = 0.8$ ms, with $\Omega_S = 0$, $\frac{\omega_{1S}}{2\pi} = 35$ kHz, and $\frac{\Delta\omega_S}{2\pi} = 110$ kHz, $\Omega_I = 0$, $\frac{\Delta\omega_I}{2\pi} = 80$ kHz, and $\frac{\omega_{1I}}{2\pi} = 90$ kHz, 70 kHz, 50 kHz, and 30 kHz. In order to depict the Hartmann–Hahn crossings, the black lines are plotted with the offsets due to sample spinning frequency of $\frac{\omega_r}{2\pi} = 13.5$ kHz. (c) Time dependence of the magnitude of the effective field in NICP for the S spin (blue lines) and I spin (black lines). Parameters are the same in (b) except for $\frac{\Delta\omega_S}{2\pi} = 0$. (For interpretation of the references to color in this figure legend, the reader is referred to the web version of this paper.)

deviation in rf intensity and spectral distribution. In this respect, SADIS CP is expected to show further advantages in experiments involving spins with large spectral distribution such as ^{19}F, ^{31}P, and paramagnetic samples.

5. Conclusions

In summary, an improved scheme for heteronuclear cross polarization, which we call as SADIS CP, has been proposed, demonstrated and analyzed. In this technique, adiabatic frequency sweep from far-off to on-resonance is employed on both the source and target spins simultaneously. As compared to the previously proposed NICP technique, which has been shown to be a special case of SADIS CP with zero frequency-sweep width on the target channel, SADIS CP keeps the Hartmann–Hahn mismatch $\Delta_{HH}(t)$ smaller throughout the sequence, allowing the faster magnetization buildup of the target spin and more robust transfer against deviation in the rf amplitudes. And yet, SADIS CP retains the favorable properties of NICP, and is thus compatible with fast sample spinning and large spectral distribution of the source spins, as discussed in our previous work [16]. Since the off-resonance irradiation on the S channel increases the magnitude of the effective field on the target spins, which can suppress the loss of magnetization due to the effect of relaxation, SADIS CP is also expected to be well applicable to experiments where either or both of the source and target spins are subjected to fast relaxation.

Acknowledgments

This work was supported by the CREST program of the Japan Science and Technology Agency and W.K.P thanks

the 21st Century Center of Excellence (COE) program for financial support.

References

[1] S.R. Hartmann, E.L. Hahn, Nuclear double resonance in the rotating frame, Phys. Rev. 128 (1962) 2042.
[2] A. Pines, M.G. Gibby, J.S. Waugh, Proton-enhanced NMR of dilute spins in solids, J. Chem. Phys. 59 (1973) 569.
[3] E.R. Andrew, A. Bradbury, R.G. Eades, Nuclear magnetic resonance spectra from a crystal rotated at high speed, Nature 182 (1958) 1659.
[4] I.J. Lowe, Free induction decays of rotating solids, Phys. Rev. Lett. 2 (1959) 285.
[5] A. Samoson, T. Tuherm, Z. Gan, High-field high-speed MAS resolution enhancement in ^{1}H NMR spectroscopy of solids, Solid State Nucl. Magn. Reson. 20 (2001) 130.
[6] A. Samoson, Encyclopedia of Nuclear Magnetic Resonance, vol. 9, Wiley, Chichester, 2002, p. 59.
[7] A. Samoson, T. Tuherm, J. Past, A. Reinhold, T. Anupold, I. Heinmaa, Top. Curr. Chem. 246 (2004) 15.
[8] S. Hediger, B.H. Meier, R.R. Ernst, Cross polarization under fast magic angle sample spinning using amplitude-modulated spin-lock sequences, Chem. Phys. Lett. 213 (1993) 627.
[9] S. Hediger, B.H. Meier, N.D. Kuru, G. Bodenhausen, R.R. Ernst, NMR cross polarization by adiabatic passage through the Hartmann–Hahn condition (APHH), Chem. Phys. Lett. 223 (1994) 283.
[10] S. Hediger, B.H. Meier, R.R. Ernst, Adiabatic passage Hartmann–Hahn cross polarization in NMR under magic angle sample spinning, Chem. Phys. Lett. 240 (1995) 449.
[11] M. Baldus, D.G. Geurts, S. Hediger, B.H. Meier, Efficient ^{15}N–^{13}C polarization transfer by adiabatic-passage Hartmann–Hahn cross polarization, J. Magn. Reson. A118 (1996) 140.
[12] S. Hediger, P. Signer, M. Tomaselli, R.R. Ernst, B.H. Meier, A combination of slow and fast RF field modulation for improved cross polarization in solid-state MAS NMR, J. Magn. Reson. 125 (1997) 291.
[13] G. Metz, X. Xiaoling, S. Smith, Ramped-amplitude cross polarization in magic-angle-spinning NMR, J. Magn. Reson. A110 (1994) 219.
[14] A.C. Kolbert, A. Bielecki, Broadband Hartmann–Hahn matching in magic-angle spinning NMR via an adiabatic frequency sweep, J. Magn. Reson. A116 (1995) 29.
[15] R. Fu, P. Pelupessy, G. Bodenhausen, Frequency-modulated cross polarization for fast magic angle spinning NMR at high fields: relaxing the Hartmann–Hahn condition, Chem. Phys. Lett. 264 (1997) 63.
[16] W.K. Peng, K. Takeda, M. Kitagawa, A new technique for cross polarization in solid-state NMR compatible with high spinning frequencies and high magnetic fields, Chem. Phys. Lett. 417 (2006) 58.
[17] S.C. Shekar, D.K. Lee, A. Ramamoorthy, Chemical shift anisotropy and offset effects in cross polarization solid-state NMR spectroscopy, J. Magn. Reson. 157 (1996) 223.
[18] F. Bloch, Dynamical theory of nuclear induction. II, Phys. Rev. 102 (1956) 104.
[19] A.E. Bennett, C.M. Rienstra, M. Auger, K.V. Lakshmi, R.G. Griffin, Heteronuclear decoupling in rotating solids, J. Chem. Phys. 103 (1995) 6951.
[20] C.G. Moreland, ^{13}C–^{13}C dipolar interactions as relaxation mechanism, J. Magn. Reson. 15 (1974) 596.
[21] R.E. London, N.A. Matwiyoff, D.D. Mueller, Spin–lattice relaxation time in an AM(X_n): application to ^{13}C relaxation in enriched molecules, J. Chem. Phys. 63 (1975) 4442.
[22] K. Akasaka, S. Ganapathy, C.A. McDowell, A. Naito, Spin–spin and spin–lattice contributions to the rotating frame relaxation of ^{13}C in L-alanine, J. Chem. Phys. 78 (1983) 3567.